Longitudinal Dispersion of Liquid Flowing Through Fixed and Fluidized Beds

S. F. CHUNG and C. Y. WEN

West Virginia University, Morgantown, West Virginia

Longitudinal liquid mixing in fluidized and fixed beds was studied using sinusoidal and pulse response techniques. The tracer used was light emissive fluorescein dye. A systematical study of liquid phase dispersion by varying particle size, fluid velocity, fraction voids, and particle density was conducted. A generalized correlation applicable to both fixed bed and fluidized bed was obtained. The application of the correlation in predicting the effect of the dispersion on reactor performance was discussed.

The study of fluid mixing in a continuous flow system is of considerable importance for the design of chemical reactors. Neglecting the fluid dispersion may result in an overestimation of the conversion, the driving force, and the volume efficiency of the system. In order to estimate the dispersion coefficient in a continuous flow reactor, the dynamic response method has been generally applied. This method involves injecting a tracer into the system according to a certain function and matching the response curve with that derived from the mathematical model. The parameters characterizing the mixing or dispersion of the fluid in the system are then evaluated from the best fitted mathematical curve.

In this work, experiments have been performed by using sinusoidal and pulse inputs of fluorescein tracer to fixed beds and fluidized beds. A systematic study of liquid phase dispersion has been conducted, particularly, the effects of particle size, fluid velocity, fraction voids, and particle density have been considered. Based on the knowledge of the effect of individual factors on the dispersion coefficient and the correlations suggested by the previous investigators, a generalized correlation valid for both fixed beds and fluidized beds has been obtained. A large number of fixed bed data and fluidized bed data from literature were also incorporated into this correlation in order to confirm its validity. This work is limited to the study of liquid phase mixing in particulate systems consisting of uniform size particles.

REVIEW

Table 1 shows a summary of the previous investigations on the longitudinal dispersion of liquid in fixed beds. Although there has been a large number of investigations on the fluid dispersion in fixed beds, only a few studies are available on the longitudinal dispersion of liquid in fluidized beds as shown in Table 2. The information obtained from the previous investigations on liquid mixing in fixed and fluidized beds have been fragmentary. So far no correlation that ties together the longitudinal dispersion in fixed beds with that in fluidized beds has been available. The usual method of correlation of the longitudinal dispersion is by plotting either the Peclet number vs. the Reynolds number, or the dimensionless dispersion group, $E_z\rho/\mu$, vs. the Reynolds, or by relating some dimensionless groups involving voidage, ϵ. For the fixed bed, plots of the Peclet number vs. the Reynolds number has been commonly employed (*10, 15, 20, 36, 37, 41, 49*). However, disagreements in the magnitude of the Peclet numbers exist among the various experimenters. This may be due to the factors that affect the experimental results (*3, 14, 16, 17, 31, 42*) such as the bed capacitance, the method of detecting, the use of irregular size particles, the variations in porosity of the bed, the status of flow, the hydrodynamic instability, the instrument lags, the injection end effects, the flow irregularities in tracer injection system, the column wall effect, the channeling, the assumption of a perfect input function and the over-simplification of the one parameter model in representing a very complex process.

The correlation equation of Ebach and White (*10*) for liquid phase fixed bed data is applicable to the low Reynolds number range ($du\rho/\mu < 100$). The sophisticated

TABLE 1. SUMMARY OF THE PREVIOUS WORK ON THE

Investigators	System: Liquid	System: Particles	Tracer	Input signal	Variables studied
Beran (3)	H_2O	sand	radioactive	pulse	fluid velocity
Bruinzeel (5)	H_2O	sand	KCl	step	fluid velocity
Cairns and Prausnitz (6)	H_2O	glass beads	KCl	step	fluid velocity column diameter, particle diameter
Carberry and Bretton (8)	H_2O	glass beads, raschig rings, berl saddles, intalox saddles	$NaNO_3$	pulse	fluid velocity, bed height, particle diameter, particle density
Danckwerts (9)	H_2O	raschig rings	red dye	step	single experiment
Ebach and White (10)	H_2O propylene glycerol-H_2O	glass beads, raschig rings, berl saddles, intalox saddles	blue dye	frequency response, pulse	fluid velocity, bed height, particle diameter, density shape, fluid viscosity
Harrison, et al. (13)	teepol water	glass beads	Xylene-Cyanol-FF	step	fluid velocity
Hennico, et al. (14)	H_2O glycerol-H_2O	glass beads, raschig rings, berl saddles	$NaNO_3$	step	fluid velocity, packing arrangement, particle diameter, particle density, bed height, fluid viscosity
Hiby (15)	H_2O, sugar solution	glass beads, raschig rings	NaCl sugar		fluid velocity, particle diameter d_t/d_p, L/d_t
Jacques, et al. (17)	H_2O glycerol-H_2O	glass beads, raschig rings, polyethylene pellets, intalox saddles	$NaNO_3$	step	the same as that of Hennico, et al.
Koump (19)	H_2O	glass beads	radioactive	step, impulse, frequency response	fluid velocity, particle diameter, bed height
Kramer and Alberda (20)	H_2O	raschig rings	NaCl	frequency response	fluid velocity
Kunigita, et al. (22)	H_2O	raschig rings	HCl	frequency response	fluid velocity
Liles and Geankoplis (27, 28)	H_2O	glass beads	β-naphthol	frequency response	fluid velocity
Miller, et al. (30, 48)	H_2O	benzoic acid tablets	benzoic acid tablets	steady state	fluid velocity, particle diameter
Miller and King (31)	H_2O	glass beads	$NaNO_3$	step	fluid velocity, particle diameter, bed height
Moon, et al. (32)	H_2O glycerol-water	glass beads, raschig rings, berl saddles	$NaNO_3$	step	fluid velocity, particle diameter, particle density, fluid viscosity
Nakanishi (34)	H_2O	glass beads	alizarin saphirol SES	frequency response	fluid velocity, particle diameter, bed height
Otake and Kunigita (35)	H_2O	berl saddles, raschig rings	NaCl	step	fluid velocity, particle diameter, particle density
Rafai (39)	H_2O	sand	salt	step	fluid velocity, bed height
Smith and Bretton (42)	H_2O	glass beads	blue dye	pulse testing	fluid velocity, bed height
Strang and Geankoplis (44)	H_2O	glass beads, porous aluminum spheres, raschig rings	β-naphthol	frequency response	fluid velocity particle diameter, porous and nonporous pellets
Stoyanovskii (43)	H_2O KI CCl_4, benzene, ethyl alcohol	glass beads	iodine	step	fluid velocity, particle diameter, bed height, fluid density

d_t, in.	d_p, in.	N_{Re}	N_{Pe}	Remarks
		0.2-4.5		
3.94-0.15		0.2-3.2	0.32-0.95	mixing cell model.
2.4	0.0513-0.126	3.5-1700	0.23-0.79	no effect of bed height. bed height: 0.466 to 2 ft. random walk model.
1.5	0.02-0.24	0.163-762	0.2-1.3	bed height: 0.5'-3'. signifiant bed height effect for bed of less than 2 ft. in length.
1.9	0.375	22	0.55	data points agree well with the F curve derived from the dispersion model.
2	0.0083-0.27	0.02-40	0.3-0.62	bed height: 3.0-5 ft. viscosity: 0.95-28 c.p. $E_z = 1.92\ d_p u^{-1.06}$ no effect of particle shape, fluid viscosity and bed height.
3.94	1.5	20-100		
2.5	0.38-0.75	3-300	0.313-1.98	random-walk model segmented laminar flow dispersion model. bed length: 1'-197'. no effect of bed height. plot of $\epsilon\ N_{Pe}$ vs. $N_{Re}/1 - \epsilon$. significant effect of viscosity at large N_{Re}.
	0.0394	1.5-20	0.8-1.0	$d_t/d_p = 2.3, 3.1, 6.3$. significant effect of d_t/d_p. a decrease in E_z when the ratio $L/d_t < 10$.
2.6	0.22-0.75	5.28-1940	0.2-2.0	random-walk model segmented laminar flow dispersion model. plot of N_{Pe} vs. $N_{Re}\ \epsilon^{1/2}$. bed length: 1-2.1 ft. wall effect is negligible at $d_t/d_p > 8$ for random packing in turbulent flow.
	0.059-0.0169	0.1-1.0		diffusion-dead space model. bed length: 0.229-2.28 ft. no effect on bed height.
2.9	0.375	75-150	0.9	mixing of the liquid is increased with increasing liquid velocity. matching data with the A.R. curve is more accurate than with the phase lag curve.
3.94	0.473	100-2000	0.65-1.3	plot of N_{Pe} vs. N_{Re}.
2.0	0.02-0.25	19-105	0.27-0.74	bed height: 0.2-5 ft. no effect of bed height.
1.97	0.127-0.274	50-500	0.63-0.05	dispersion model, cell model. plot of $E_z\rho/\mu$ vs. N_{Re}.
0.5	0.0051-0.14	0.0035-36	0.32-0.7	bed height: 5.5, 11, 22 in. no significant effect of particle size, d_t/d_p, and the bed height on the plot of N_{Pe} vs. $N_{Re}/1 - \epsilon$ on log-log scale.
6.25	0.65-0.76	20-300	0.11-2.0	dispersion model, random-walk model. significant effect of viscosity.
2.36	0.0866-0.22	7-173	0.311-0.68	plot of N_{Pe} vs. N_{Re}, E_z vs. u. significant effect of particle size. no effect of bed height.
1.61-2.64	0.272-0.61	50-10^3		$\frac{uL}{2E_z} \propto d_p^{-3/2}\, u_o^{-1/2}\, L.$
		1	0.3-0.55	
1.5	0.0394-0.118	10-10^3	0.008-1.1	bed height: 1-7 ft. significant bed capacitance effect for the long bed with small particles.
1.65	0.23-0.27	5-33.6	0.4-1.6	plot of N_{Pe} vs.N_{Re}, E_z vs. u. bed height: 1.25-1.9 ft. large fluid velocity effect on E_z.
1.04	0.0295-0.256	0.1-20		bed height: 1.6-6.55 ft. dispersion coefficient is proportional to fluid velocity and particle diameter and decreases with increasing column diameter. no bed height effect. no effect of density, viscosity, and surface tension of the fluids, except CCl_4 gives higher E_z.

Table 2. Summary of the Previous Work on the

Investigators	Liquid	System Particles	Tracer	Input signal	Variables studied
Bruinzeel, et al. (5)	H_2O	sand	$NaNO_3$	step	fluid velocity, particle diameter, column diameter, bed height
Cairns and Prausnitz (7)	H_2O	glass beads, lead beads	$NaNO_3$	step	fluid velocity, particle diameter, particle density, column diameter
Kramer, et al. (21)	H_2O	glass beads	KCl	step	fluid velocity, particle diameter, void fraction
Miller, et al. (30, 48)	H_2O	benzoic acid	benzoic acid	steady state	fluid velocity, particle diameter
Muchi, et al. (33)	H_2O	sand	HCl	steady state	fluid velocity, particle diameter, column diameter
Nakanishi (34)	H_2O	glass beads	alizarin saphirol SES	frequency response	fluid velocity, bed height
Shemilt (40)	H_2O	glass, resin, steel beads	NaCl	pulse testing	fluid velocity, particle diameter, particle density
Wakao (46)	H_2O	β-naphthol	β-naphthol	steady state	fluid velocity, particle diameter, void fraction

analysis of liquid dispersion in fixed beds of laminar flow range given by Perkins, et al. (36) requires specific information, such as the inhomogeneity factor and the formation electrical resistivity factor for which the exact data are not easily obtained. Extrapolation of the correlation equations proposed by Muchi, et al. (33) and Bruinzeel, et al. (15) for liquid phase fluidized bed to the velocity range near the minimum fluidization point does not satisfactorily agree with the fixed bed data. Miller, et al. (30, 48) and Nakanishi (34) obtained straight line relationships for fluidized bed data on log-log plots of $E_z\rho/\mu$ vs. N_{Re} and N_{Pe} vs. N_{Re} respectively for single size particles. They did not study systematically the effects of particle size and particle density on liquid dispersion.

MATHEMATICAL MODEL

The longitudinal dispersion of the fluid in fixed beds and fluidized beds are considered to be composed of the molecular diffusion, the turbulent diffusion, and the convective diffusion caused by a nonuniform velocity distribution. An early study by Taylor (45) on the dispersion of a tracer material in a cylindrical pipe has shown that the flow of the tracer in a tube is described by dispersion due to molecular diffusion accompanied by the radial velocity variations. It may be approximated by a flow with a flat velocity profile equaling the mean velocity with an effective longitudinal dispersion coefficient. This is the so-called "longitudinal dispersed plug flow model" or simply the "dispersion model". The radial liquid phase dispersion can be neglected in comparison with the axial dispersion for small ratio of column diameter to length and large fluid velocity as discussed by Klinkenberg (18) and Bruinzeel, et al. (5). The assumption of flat velocity profile in a fixed bed is reasonable when d_t/d_p is greater than 15 as pointed out by Akehata and Sato (2). A material balance of an infinitesimal length of the packed column results in a differential equation,

$$\frac{\partial c}{\partial t} = E_z \frac{\partial^2 c}{\partial z^2} - u \frac{\partial c}{\partial z} \tag{1}$$

where E_z is an effective longitudinal dispersion coefficient, based on the interstitial velocity, u. The boundary conditions are

$$(1)\ uc_i = uc_{z\to 0+} - E_z \left(\frac{\partial c}{\partial z}\right)_{z\to 0+} \tag{2}$$

$$(2)\ \frac{\partial c}{\partial z} = 0 \qquad \text{at } z = L \qquad \text{for all } t \tag{3}$$

A steady state solution of Equation (1), with a first-order irreversible chemical reaction and with the above boundary conditions, was obtained by Langmuir (23) as early as 1908 and later by Danckwerts (9). The amplitude ratio and phase shift due to frequency response of this model were derived by Fan and Ahn (1, 11, 12) as

$$\text{A.R.} = \frac{be^M}{(\alpha_1^2 + \alpha_2^2)^{1/2}} \tag{4}$$

and

$$\Phi = -\tan^{-1}\left(\frac{\alpha_2}{\alpha_1}\right) + a \tag{5}$$

where

$$M = uL/2E_z, \text{ a mixing parameter} \tag{6}$$

$$\theta = L/u, \text{ residence time} \tag{7}$$

$$a = 1/2 \tan^{-1}\left(\frac{2\omega\theta}{M}\right) \tag{8}$$

$$b = \left[1 + \frac{4(\omega\theta)^2}{M^2}\right]^{1/4} \tag{9}$$

$$\alpha_1 = \sinh x \cos y - \frac{\omega\theta}{M}\cos h\, x \sinh y + b(\cos a \cosh x \cos y - \sin a \sinh x \sin y) \tag{10}$$

$$\alpha_2 = \frac{\omega\theta}{M}\sinh x \cos y + \cosh x \sin y + b(\cos a \sinh x \sinh y + \sin a \cosh x \cos y) \tag{11}$$

d_t, in.	d_p, in.	N_{Re}	N_{Pe}	Remarks
0.0394-0.394	0.00197-0.0197	0.372-14.5	0.00114-0.0198	mixing cell model. $N_{Pe} \propto N_{Re}^{0.18}$ no effect of the diameter of the bed.
2, 4	0.05, 2, 0.118, 0.126		10^{-2}-10	the longitudinal mixing is strongly affected by particle concentration. longitudinal dispersion coefficient increases with particle density and with decreasing d_p/d_t.
1, 1.39	0.0197-0.0394	5.7-105	0.09-0.23	plots of u vs. ϵ, E_z vs. ϵ. straight line relation between u and ϵ on log-log scale.
1.97	0.152-0.224	66-523	0.04-0.3	a straight line relation between $E_z\rho/\mu$ vs. N_{Re} on log-log scale.
2.64, 3.9, 4.79	0.0079-0.0474	2-30	0.005-0.117	dispersions on longitudinal and radial directions were considered simultaneously for the shallow beds. $E_z\rho/\mu = 70(N_{Re}/1 - \epsilon)^{0.5}$
2.36	0.059	10-51	0.04-0.959	a straight line relation between N_{Pe} and N_{Re}. the use of screen as a distributor gave higher mixing than the use of a perforated plate as the distributor.
2	0.0197-0.118			for a given bed voidage, mixing increased with particle size. good agreement between the data and the dispersion model.
2	0.26-0.3	260-290	0.0634-0.386	E_z increased with the increase of ϵ, and reached the maximum value at $\epsilon = 0.8$.

and

$$x = Mb \cos a \quad (12)$$

$$y = Mb \sin a \quad (13)$$

EXPERIMENTAL PROCEDURE

Solid particles were packed in a 2 in. diam. glass column. The glass column was light insulated except at the upper test section and the lower test section. Each section provides two windows located at the same level but at an angle of 120°. One window receives the light from a light bulb. The light emissive tracer, sodium salt of fluorescein, in the glass column emits light and passes through the second window to the phototube. The phototube transforms the light intensity of the tracer solution to the intensity of electrical current. A recorder records the current passed through the phototube which in turn is converted into the variation of the concentration of the tracer solution with respect to time. The tracer concentration measured in this way is the cross-sectional mean concentration.

Before performing the experiment, special care must be exercised to remove all the air bubbles in the column and the pipe line. The existence of the air bubbles not only influence the light intensity measurement, but also cause local particle agglomeration in fluidized beds. The resistance of the power rheostat must be adjusted so that the amplitude ratio at very low frequency is unity.

A function generator was used to generate sine current which was converted to pressure fluctuation by a transducer. The pneumatic pressure mechanically forced the needle valve opened and closed sinusoidally. Tracer was stored in a pressure tank under an air pressure. For each run a different amount of the uniform size particles was introduced into the column through a valve at the top. The fluidized bed was always expanded to 2 ft. 8 in., the full test section length, by adjusting the flow rate. Schematic diagrams of the equipment and the tracer concentration recording system are shown in Figures 1 and 2.

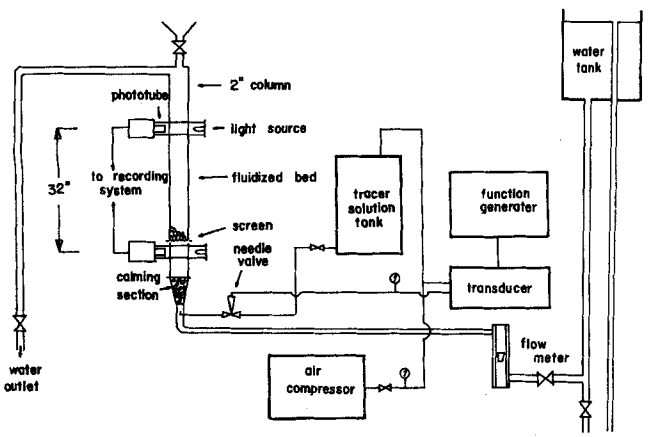

Fig. 1. Schematic diagram of the equipment for frequency response on liquid fluidization system.

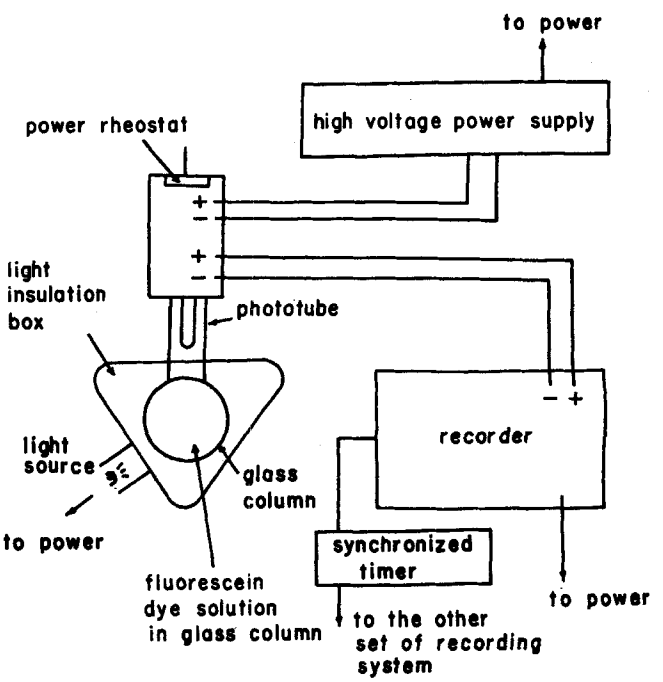

Fig. 2. Schematic diagram of the tracer concentration recording system.

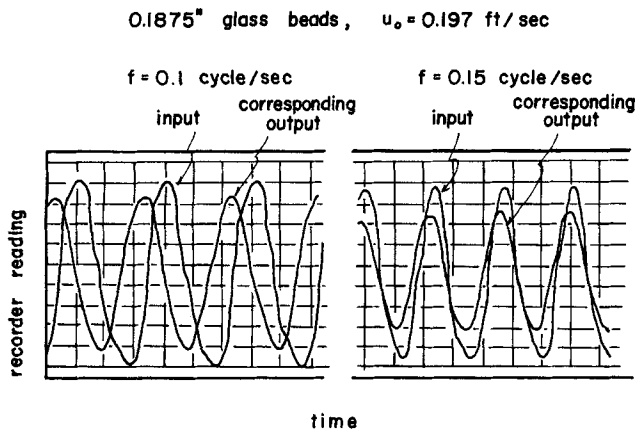

Fig. 3. A strip chart from recorder showing sinusoidal tracer concentration waves.

Tracer

The tracer used is the sodium salt of fluorescein having the chemical name of *di*-sodium salt of 9-0-carboxy-phenyl-6-hydroxy-3-isoxanthone ($Na_2C_{20}H_{10}O_5$). The wave length of light transmitted by the tracer solution is in the range of 5,100 to 8,000Å. The percentage of the incident light transmitted was measured at different wave lengths by spectrometer. The maximum light of this tracer solution transmitted is at the wave length of 5,750Å, corresponding to yellow color wave length. The reading of the miliamper scale on the recorder is linearly proportional to the dye concentration at low concentration range. The concentration range used was about the order of 10^{-3} g./liter. At higher concentrations the relation between the recorder reading and the dye concentration may not be linear, requiring calibration for high concentration range.

No data on the molecular diffusivity of this particular dye at low concentration range are available in literature. However, the molecular diffusivity of this dye measured by the light defraction method was found to be about 1.5×10^{-5} sq.cm./sec. at high concentrations.

It was found that fluorescein dye is a very satisfactory tracer. Since the tracer is completely miscible with water, and has high sensitivity at a very low concentration range the dye solution has the similar physical properties as the main fluid stream. Therefore, the injection of a small amount of dye solution does not affect the hydrodynamic properties and the mixing pattern of the main stream. Furthermore, the tracer is inexpensive, and no adsorption of the dye solution to the particles was observed.

SUMMARY OF EXPERIMENTS

System: water.

Tracer: fluorescein dye.

Variable studied: fluid velocity, particle size, particle density, expansion ratio.

Particles: glass beads, aluminum beads, steel beads.

Range of particle diameter: 0.08 in. to 0.25 in.

Column diameter: 2 in.

Length of test section: 2 ft. 8 in.

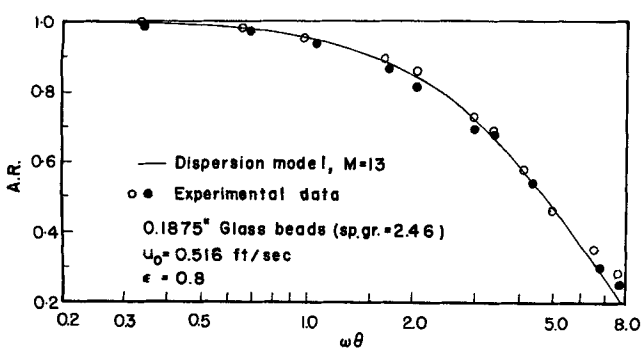

Fig. 4. Bode plot of amplitude ratio vs. $\omega\theta$ for experimental data of runs D-2 and D-3.

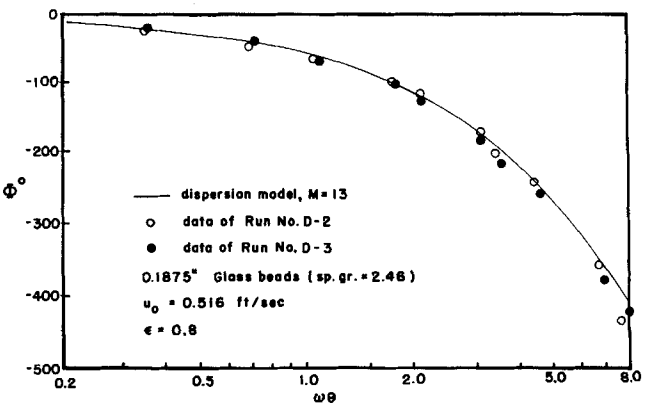

Fig. 5. Bode plot of phase shift vs. $\omega\theta$ for experimental data of runs D-2 and D-3.

Height of packing: 1 ft. to 2 ft. 8 in.

Range of Reynolds number: fixed beds: 25 to 320, fluidized beds: 51 to 1286.

Range of Peclet number: fixed beds: 0.362 to 1.025, fluidized beds: 0.1 to 0.909.

FREQUENCY RESPONSE

The dispersion coefficient is obtained by constructing a Bode plot from the frequency response data and by matching it with the theoretical curves obtained from the dispersion model. A proper parameter, M, is then chosen by the least square fitting. Figure 3 shows a typical recording of sinusoidal tracer concentration waves. Figures 4 and 5 show an example of the Bode plot (in amplitude ratio and phase shift) indicating the closeness of matching the experimental data with the theoretical curve derived from the dispersion model. The standard deviation of the amplitude ratios between the dispersion model and the experimental data for this run is 5.16%. The average deviation of all of the experimental runs is about 4.5% with the maximum deviation of 9.1%. Figures 4 and 5 also show a comparison of the amplitude ratios of the duplicated experimental runs. The data between these duplicated runs are in sufficient agreement.

Pulse signals were also used to obtain the longitudinal dispersion coefficients. By the method of Fourier analysis, the pulse response data are used to obtain amplitude ratios and phase shifts. An example is shown in Figure 6 which compares the converted pulse testing data with the sinusoidal testing data in frequency domains. The average standard deviation between these two methods for all of the experimental runs is estimated to be 5%

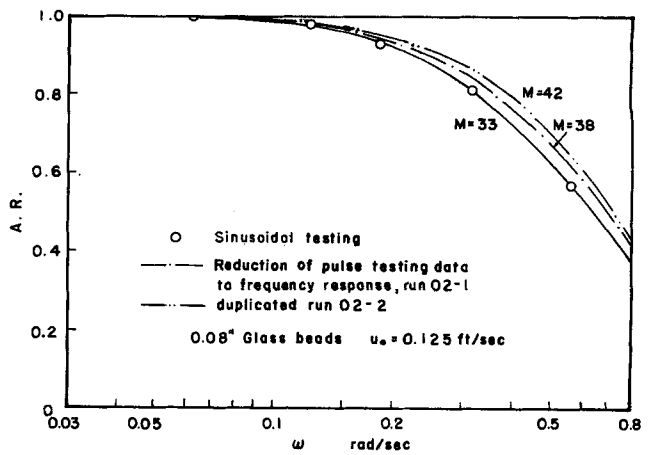

Fig. 6. Comparison of the sinusoidal testing data with the duplicated pulse testing data of run O-2 in frequency domain.

with the largest deviation of 17.5% as shown in Figure 6.

CORRELATION AND DISCUSSION

The effect of fluid velocity on the dispersion coefficients of fixed beds and fluidized beds is shown in Figure 7. An increase in the velocity increases the dispersion coefficient, especially for fluidized beds. A considerable particle size effect is observed on the log-log plot of E_z vs. u_o for fixed bed data, but much less effect is seen for the fluidized bed data of constant particle density. The slope of the fixed bed data on the $E_z\rho/\mu$ vs. $d_p u_o \rho/\mu$ plot on log-log scale is approximately 1 at the small Reynolds number range ($N_{Re} < 40$) and is less than 1 at the large Reynolds number range. ($N_{Re} > 40$). This has been pointed out by Ebach and White (*10*). A plot of log $E_z\rho/\mu$ vs. log N_{Re} incorporating available fluidized bed data in literature (*30, 33, 34, 46*) is shown in Figure 8. A few interesting facts are noted: (a) an increase in the fluid velocity (or Reynolds number) of the fixed bed of uniform size particles accompanies an increase in the dispersion coefficient (or $E_z\rho/\mu$). Beyond the minimum fluidization point, the increase of the dispersion coefficient with respect to the velocity becomes very rapid. (b) log $E_z\rho/\mu$ is linearly proportional to log N_{Re} for the fluidized bed data. The slopes of the lines for particles having the similar densities are approximately the same. Cairns, *et al.* (7) reported that lead spheres have a higher slope than that of glass beads. (c) Each straight line can be represented by a Galileo number. The minimum fluidization Reynolds number is related to the Galileo number by the following equation (*47*):

$$(N_{Re})_{mf} = \sqrt{(33.7^2 + 0.0408\, N_{Ga})} - 33.7 \qquad (14)$$

The minimum fluidization points for different particles can be connected by one curve on the log $E_z\rho/\mu$ vs. log N_{Re} plot. The Galileo number, the calculated $(N_{Re})_{mf}$ and the experimental $(N_{Re})_{mf}$ are listed in Table 3.

Although the fixed bed data from literature are rather scattered, a correlation of both the fixed bed and fluidized bed data is believed possible. Since, in a particulate fluidization, each particle may be considered to be freely suspended, a liquid fluidized bed may be approximated by a fixed bed with a large void fraction. The bed expansion may be related to the ratio $(N_{Re})_{mf}/N_{Re}$. Thus, a plot of the product, $\epsilon N_{Pe}/[(N_{Re})_{mf}/N_{Re}]$ vs. N_{Re} on log-log scale for the fluidized bed data was made. An examination of this plot reveals that all the fluidized bed data points seem to fall on the correlation line of the fixed bed data when ϵN_{Pe} is plotted vs. N_{Re}. Thus, as shown in Figure 9, a plot of $\epsilon N_{Pe}/X$ vs. N_{Re} on log-log scale for both the fixed bed data and the fluidized bed data was constructed. Here, X equals 1 for fixed bed data and equals $(N_{Re})_{mf}/N_{Re}$ for fluidized bed data.

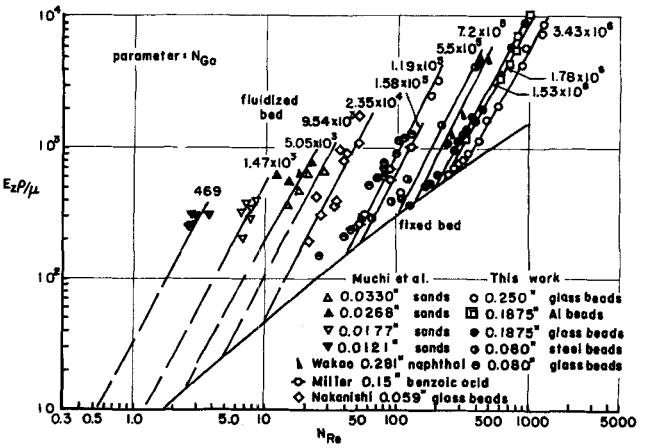

Fig. 8. Dimensionless dispersion group vs. Reynolds number for fixed bed and fluidized bed data (liquid phase).

TABLE 3. LIST OF THE GALILEO NUMBER, CALCULATED AND EXPERIMENTAL MINIMUM FLUIDIZATION REYNOLDS NUMBERS FOR FLUIDIZED BEDS

Investigators	Particles	d_p, in.	N_{Ga}	$(N_{Re})_{mf}$, cal.	$(N_{Re})_{mf}$, exp.
This work	glass	0.25	3.4×10^6	330	320
	aluminum	0.1875	1.78×10^6	237	—
	glass	0.1875	1.53×10^6	218	208
	steel	0.08	5.5×10^5	119	109
	glass	0.08	1.19×10^5	43	45
Wakao, et al. (*46*)	naphthol	0.281	7.2×10^5	130	125
Miller, et al. (*30, 48*)	benzoic acid	0.15	1.58×10^5	53	50
Muchi, et al. (*33*)	sand	0.033	9.54×10^3	5.79	4.9
		0.0268	5.05×10^3	3.0	2.68
		0.0177	1.47×10^3	0.89	0.93
		0.0121	469	0.284	0.25
Nakanishi (*34*)	glass	0.059	2.35×10^4	12	10.0

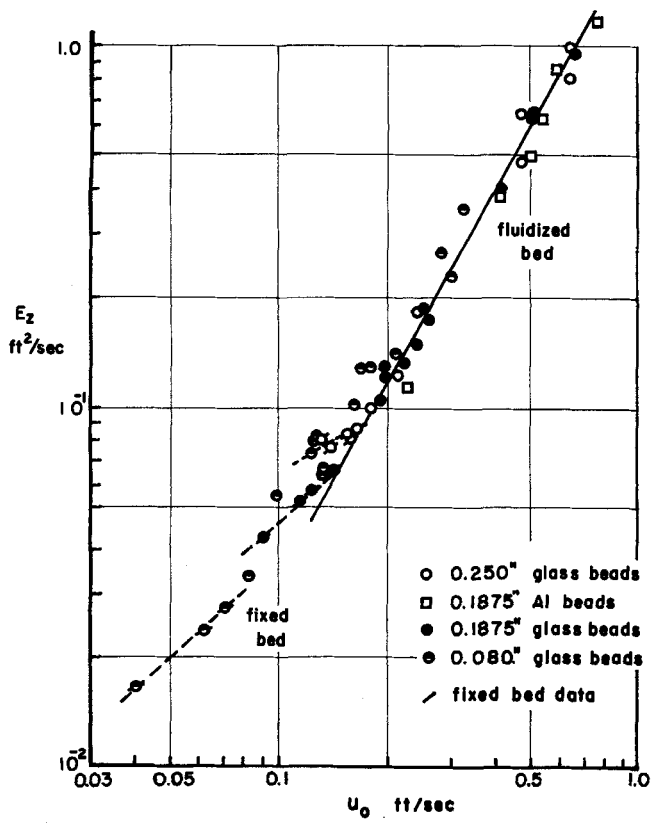

Fig. 7. Effect of fluid velocity on dispersion coefficient of fixed beds and fluidized beds of constant particle density.

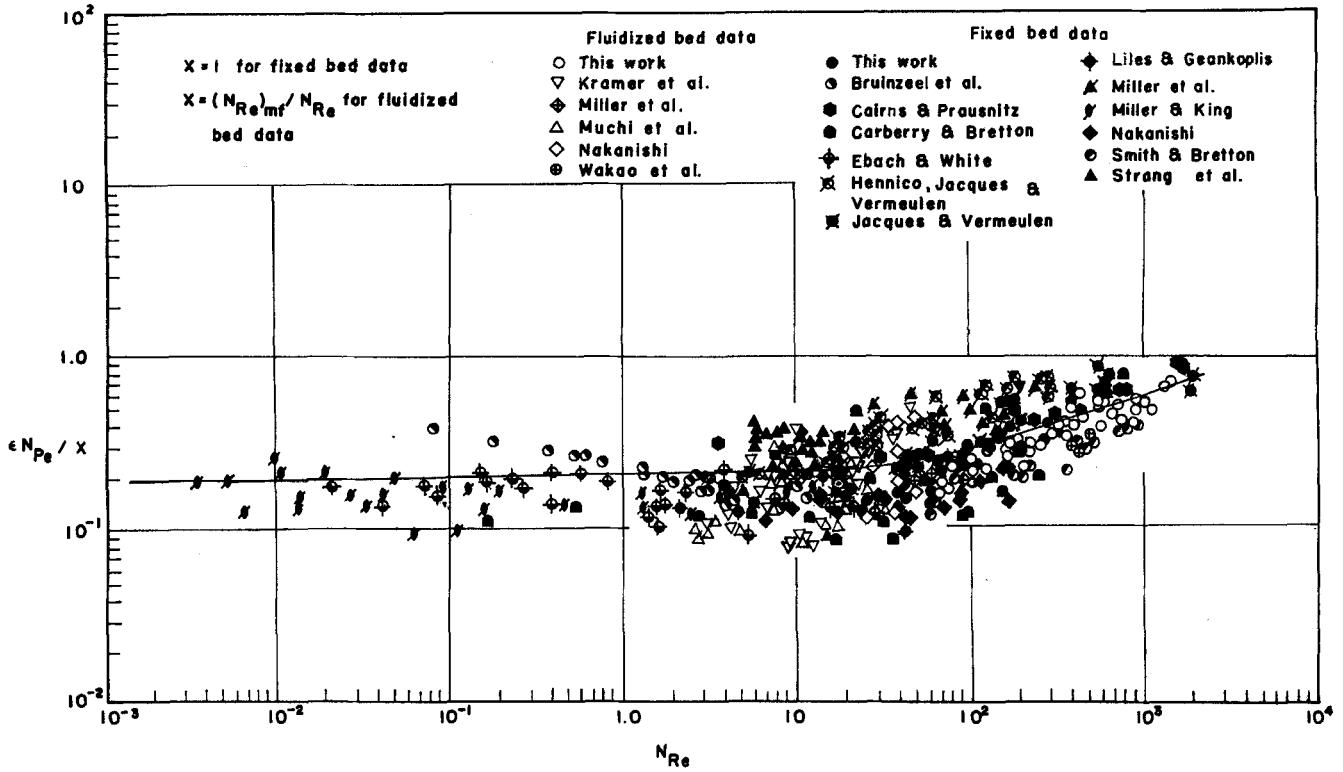

Fig. 9. Correlation of longitudinal dispersion coefficients of liquid phase fixed beds and fluidized beds in terms of Peclet number.

The Peclet number can be directly related to the mixing parameter, M, conveniently. The correlation equation can be expressed as

$$\epsilon N_{Pe}/X = 0.20 + 0.011\, N_{Re}^{0.48} \qquad (15)$$

Equation (15) can be rearranged to give

$$\frac{E_z\rho}{\mu}(X) = \frac{N_{Re}}{0.20 + 0.011\, N_{Re}^{0.48}} \qquad (16)$$

The standard deviation of the correlation equation based on 482 available data points is 46%. Equations (15) and (16) are applicable in the Reynolds number range from 10^{-3} up to 10^{3}. At the lowest Reynolds number, 10^{-3}, $E_z\rho/\mu$ is in the order of 10^{-2}. The reciprocal of Schmidt number, $D\rho/\mu$, for liquid system is in the order of 10^{-3} to 10^{-4}. This is much less than the corresponding $E_z\rho/\mu$ value of 10^{-2}. Therefore, the molecular diffusion is not important even at very low Reynolds number range of 10^{-3}.

In view of the variety of the data used, the correlation must be considered satisfactory and covers the range of fraction voids from 0.4 to 0.8 and the particle density range up to 480 lb/cu. ft.

APPLICATION

As an application using the developed correlation, the effect of liquid dispersion on the reactor performance may be demonstrated. In reactor design, the conversion can be related with the volume ratio of the actual reactor to the plug reactor (25, 38) and the mixing parameter is related to the Peclet number by

$$M = N_{Pe}\frac{L}{2d_p}$$

where d_p is particle diameter and L the bed height. Based on these relationships, the effect of the longitudinal dispersion in a fixed bed and in a fluidized bed as a function of the flow rate can be obtained. First, let us consider a constant volume reactor in which the fluid velocity is varied so that the reactor is operated from the fixed bed condition to the fluidized bed condition. In evaluating the effect of dispersion in this reactor, a plug flow reactor having the some volume (or residence time) as that of the fixed or fluidized bed reactor is compared. This is shown in terms of c_A/c_{Ap} in Figure 10. Next, we consider a case in which the conversion in the plug flow reactor is the same as that in the fixed or fluidized bed reactor at the same Reynolds number. This is shown in terms of V/V_p in Figure 11. It is interesting to note that the minimum V/V_p or c_A/c_{Ap} occurs at about the minimum fluidization point. In the fixed bed region, an increase of N_{Re} causes a decrease in θ or R, thus decreases c_A/c_{Ap} or V/V_p. However, in the fluidized bed region, the Peclet number decreases so rapidly with an increasing N_{Re} that the overall effect is to increase the value of c_A/c_{Ap} or V/V_p as N_{Re} increases. The fluidized bed curves in Figures 10 and 11 were extended to the Reynolds number correspond-

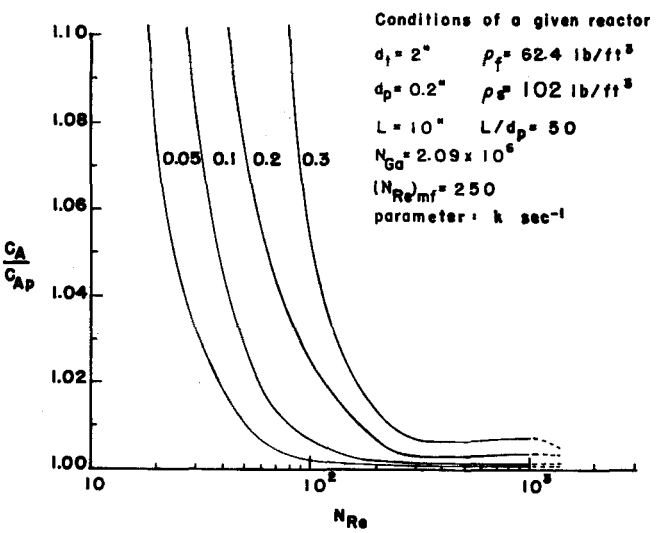

Fig. 10. Example of the variation of c_A/c_{Ap} vs. Reynolds number based on identical volumes of a given reactor and a plug flow reactor.

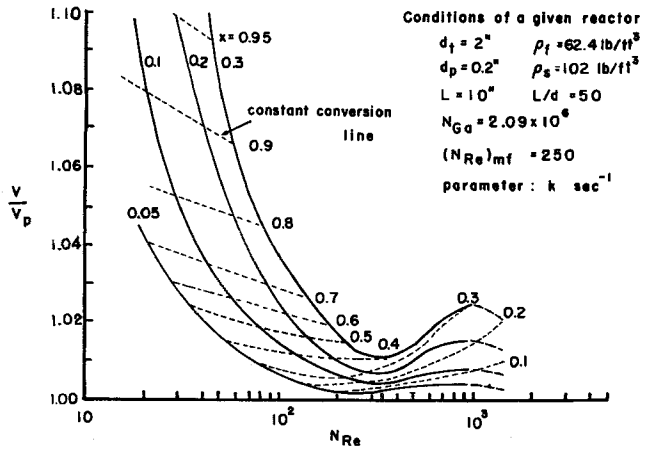

Fig. 11. Example of the variation of V/V_p vs. Reynolds number based on identical conversions in a given reactor and a plug flow reactor.

ing to the terminal velocity of the particles ($\epsilon = 1.0$) by using the dispersion coefficient estimated from the correlation for fluid flowing in pipes (*24*).

CONCLUSION

A large number of experimental data including those available in literature for fixed and fluidized beds covering a wide Reynolds number range were examined and correlated. Fluid velocity is found to have a strong influence on the longitudinal dispersion coefficient. An increase in the velocity causes an increase in the dispersion coefficient. The increase in the dispersion coefficient is particularly significant after the onset of fluidization. Data obtained from the sinusoidal testing agree well with those obtained from the pulse testing method.

The dispersion coefficient of liquid flowing through the fixed and fluidized bed can be correlated by a plot of $\epsilon N_{Pe}/X$ vs. N_{Re} on log-log scale as shown in Figure 9. A generalized correlation equation applicable for both a fixed and fluidized bed is proposed as given in Equation (15) or (16). The correlation is applicable in the range of fraction voids from 0.4 to 0.8 with particle density up to 480 lb./cu.ft. and Reynolds number range from 10^{-3} to 10^3. For the Reynolds number less than 10, the value of $\epsilon N_{Pe}/X$ is approximately 0.2. A transition region occurs over the range of N_{Re} from 10 to 10^3. At $N_{Re} > 10^3$ the values of $\epsilon N_{Pe}/X$ approaches 0.8. This value agrees with the theoretical value of $N_{Pe} = 2$ for a fixed bed, based on the assumption that the bed acts as a series of n perfect mixers, where n is the number of particles traversed between inlet and outlet (*29*).

It is of interest to note that the minimum V/V_p or c_A/c_{Ap} for a first order reaction system in a given length column occurs approximately at the fluidization point.

ACKNOWLEDGMENT

The authors wish to acknowledge the support of this work by the National Science Foundation Grant GP-560.

NOTATION

a = angle defined as in Equation (8), degree
A.R. = amplitude ratio, dimensionless
b = constant defined as in Equation (9), dimensionless
c = concentration, Moles/L³
D = molecular diffusivity, L^2/t
d_p = particle diameter, L
E_{oz} = effective longitudinal dispersion coefficient, based on superficial velocity, L^2/t
E_z = effective longitudinal dispersion coefficient, based on interstitial velocity, L^2/t
g = gravitational acceleration, L/T^2
N_{Ga} = $[d_p^3\ \rho(\rho_s - \rho)g]/\mu^2$, Galileo number, dimensionless
k = first-order reaction rate constant, $1/t$
L = length, L
M = $uL/2E$, dimensionless
N_{Pe} = $(d_p u)/E_z = (d_p u_o)/E_{oz}$, Peclet number, dimensionless
R = $k\theta$, first order reaction rate group, dimensionless
N_{Re} = $(d_p u_o \rho)/\mu$, Reynolds number, dimensionless
t = time, t
u_o = superficial velocity, L/t
u = interstitial velocity, L/t
X = 1, for fixed bed data, = $(N_{Re})_{mf}/N_{Re}$ for fluidized bed data, dimensionless
x = conversion
z = length, longitudinal direction, L

Greek Letters

α_1 = constant, defined as in Equation (10)
α_2 = constant, defined as in Equation (11)
ϵ = voidage, dimensionless
θ = L/u, residence time, t
μ = viscosity of fluid, M/Lt
ρ = density of fluid, M/L^3
σ = standard deviation
ϕ = phase shift, radian or degree
ω = angular frequency, rad./t

Subscripts

b = bed
i = inlet
mf = minimum fluidization
o = outlet, superficial
p = plug flow reactor
s = solid particle
z = longitudinal direction

LITERATURE CITED

1. Ahn, Y. K., MS thesis, Kansas State Univ., Manhattan (1962).
2. Akehata, T., and K. Sato, *Chem. Eng. (Japan)*, **22**, 430 (1958).
3. Beran, M., Ph.D. dissertation, Harvard Univ., Cambridge, Mass. (1955).
4. Bischoff, K.B., Ph.D. dissertation, Illinois Inst. Tech., Chicago (1961).
5. Bruinzeel, C., G. H. Reman, and E. Th. van Der Laan, Third Congr. European Federation Chem. Eng., Olympia, London (June, 1962).
6. Cairns, E. J., and J. M. Prausnitz, A. *Chem. Eng. Sci.*, **12**, 20 (1960).
7. ———, *AIChE J.*, **6**, 400 (1960).
8. Carberry, J. J. and R. H. Bretton, *ibid.*, **4**, 367 (1958).
9. Danckwerts, P. V., *Chem. Eng. Sci.*, **2**, 1 (1955).
10. Ebach, E. A. and R. R. White, *AICHE J.*, **4**, 161 (1958).
11. Fan, L. T. and Y. K. Ahn, *Digest Joint Automatic Control Conference*, Boulder, Colorado (1961).
12. ———, *Chem. Eng. Progr., Symp. Ser., No. 46*, **59**, 91 (1963).
13. Harrison, D., et al., *Trans. Inst. Chem. Engrs.*, **40**, 214 (1962).
14. Hennico, A., G. Jacques, and T. Vermeulen, *UCRL 10696* (1963).
15. Hiby, J. W., *Proc. Symp. Interaction Fluid Solid Inst. Chem. Eng., (London)*, 312 (1962).
16. Ichikawa, A., and G. Kawata, *30th Annual Meeting, Chem. Engrs.*, Japan (Apr., 1965).
17. Jacques, G. L. and T. Vermeulen, *UCRL 8029* (1958).
18. Klinkenberg, A., *Ind. Eng. Chem.*, **45**, 1202 (1955).
19. Koump, V., Engr. D. thesis, Yale Univ., New Haven, Conn. (1959).

20. Kramers, H. and G. Alberda, *Chem. Eng. Sci.*, **2**, 173 (1953).
21. Kramers, H., M. D. Westermann, J. H. de Groot, and F. A. F. Dupont, paper presented at the Third Congress of the European Federation of Chem. Eng., Olympia, London, (June, 1962).
22. Kunigita, E., et al., *Chem. Eng. (Japan)*, **26**, 800, (1962).
23. Langmuir, I., *J. Amer. Chem. Soc.*, **30**, 1742 (1908).
24. Levenspiel, O., *Ind. Eng. Chem.*, **50**, 343 (1958).
25. ———, and K. B. Bischoff, *ibid.*, **51**, 1431 (1959).
26. Li, N. N. and E. N. Ziegler, *ibid.*, **59**, 30 (1967).
27. Liles, A. W., Ph.D. dissertation, Ohio State Univ., Columbus (1959).
28. ———., C. J. Geankoplis, *AIChE J.*, **6**, 591 (1961).
29. McHenry, K. W., and R. H. Wilhelm, *ibid.*, **3**, 83 (1957).
30. Miller, E., MS thesis, West Virginia Univ., Morgantown, W. Va. (1961).
31. Miller, S. F., and C. J. King, *AIChE J.*, **12**, 767 (1966).
32. Moon, J. S., et al., *UCRL 10928* (1963).
33. Muchi, I., T. Mamuro, and T. Saski, *Chem. Eng. (Japan)*, **25**, 747 (1961).
34. Nakanishi, K., Ph.D. dissertation, Tohoku Univ., Sendi, Japan (1966).
35. Otake, T., and E. Kunigita, *Chem. Eng. (Japan)*, **22**, 144 (1958).
36. Perkins, T. K., and O. C. Johnston, *Soc. Pet. Engrs. J.*, **3**, 70 (1963).
37. Petersen, E. E., "Chemical Reaction Analysis," Prentice-Hall, Englewood Cliffs, New Jersey (1965).
38. Raines, G. E., and T. E. Corrigan, paper presented at AIChE. Detroit meeting, Michigan, (Dec., 1966).
39. Rafai, M.E., Ph. D. dissertation, Univ. California, Berkeley (1956).
40. Shemilt, L. W., and P. R. Krishnaswamy, 16th Canadian Chem. Eng. Conference, Windsor, Ontario, (Oct., 1966).
41. Sinclair, R. J., and O. E. Potter, *Trans. Instr. Chem. Engrs.*, **43**, 73 (1965).
42. Smith, W. D., Jr., and R. H. Bretton, paper presented at AIChE Houston Meeting, Texas (Feb., 1967).
43. Stoyanovskii, I. M., *J. Appl. Chem. USSR*, (Engl. Transl.), **34**, 1863 (1961).
44. Strang, D. A., and C. J. Geankoplis, *Ind. Eng. Chem.*, **50**, 1305 (1958).
45. Taylor, G. I., *Proc. Roy. Soc. (London)*, **A219**, 186 (1953).
46. Wakao, N., T. Oshima, and S. Yagi, *Chem. Eng. (Japan)*, **22**, 786 (1958).
47. Wen, C. Y. and Y. H. Yu, *Chem. Eng. Progr., Symp. Ser. 62*, **62**, 100 (1966).
48. ———, E. Miller, and L. T. Fan, paper presented at Am. Chem. Soc. meeting, Chicago, Ill., (Sept. 1961).
49. Wilhelm, R. H., *Pure Applied Chem.*, **5**, 403 (1962).

Manuscript received July 11, 1967; revision received November 25, 1967; paper accepted November 28, 1967. Paper presented at AIChE New York City meeting.

Sinusoidal and Pulse Response of a Plate Distillation Column by Reflux Upset

PASQUALE A. MARINO, ANGELO J. PERNA, and LEROY F. STUTZMAN

University of Connecticut, Storrs, Connecticut

A study was made to evaluate pulses as a forcing function on a 24-plate distillation column. Pulses of two shapes, rectangular and displaced cosines, and of different widths were used as inputs to the reflux return line from the condenser to the column. The effect of the disturbance was a change in the liquid return rate which correspond to the shape and size of the pulse. The output responses of the system were temperatures measured at different times and at different plates in the column.

Bode diagrams were plotted from the experimentally determined data. From these plots, it was determined that the system could be approximated by linear first-order equations. The time constants for the linear system were determined both by direct sinusoidal forcing and by pulse forcing. Pulse data were considered acceptable when the values of the time constant and the phase angle determined by the pulse compared favorably with those determined by steady state sinusoidal forcing.

The application of pulse inputs to determine the dynamic response of a chemical process system is a known technique in the chemical and petroleum industries. From a theoretical standpoint, the technique makes it possible to define the frequency response over the entire frequency range for a system with the use of a single pulse. This has been demonstrated by Dreifke (*1*), and Clements and Schnelle (*2*) through the analytical analysis of various mathematical models which they subjected to different pulses readily determined. From such studies one can see some of the advantages as well as disadvantages of pulse techniques relative to other methods of analysis such as direct frequency response by sinusoidal forcing or transient response.

When dealing with a complex chemical process or chemical operation, one is confronted with two problems which do not exist with theoretical mathematical models. One, the complete model of the system is rarely known. Further, whereas a pulse of a specified size or shape may not change the model of a theoretically defined system, it may change that of a real system. As an example, the model of a distillation column has been found to be linear (or pseudolinear) at steady state, yet, if disturbed by a large upset, it may become nonlinear during a transient

Pasquale A. Marino, is at the University of Rhode Island, Kingston, Rhode Island and Angelo J. Perna is at Newark College of Engineering, Newark, New Jersey.